Available online at www.sciencedirect.com
ScienceDirect
Ceramics International 37 (2011) 1843–1850
CERAMICS INTERNATIONAL
www.elsevier.com/locate/ceramint

Microstructural and phase transformations during sintering of a phillipsite rich zeolitic tuff

Sibel Ergul [a], Giuseppe Sappa [a,*], Donatello Magaldi [c], Paola Pisciella [b], Mario Pelino [b]

[a] Dipartimento di Ingegneria Civile, Edile ed Ambientale, Sapienza- Università di Roma, Via Eudossiana, 18, 00186, Rome, Italy
[b] Dipartimento di Chimica, Ingegneria Chimica e Materiali, Via Campo di Pile, Zona Industriale di Pile, 67100 L'Aquila, Italy
[c] Dipartimento di Scienza del Suolo e Nutrizione della Pianta, Università di Firenze,Piazzale delle Cascine, 50 144 Firenze, Italy

Received 23 June 2010; received in revised form 2 January 2011; accepted 4 February 2011
Available online 8 April 2011

Abstract

Microstructural and phase transformations during sintering of a Phillipsite rich zeolitic tuff, from Tenerife, Canary Islands, was investigated in order to their utilization in ceramic manufacturing industries. Green samples were obtained from powders and pressed at 150 MPa and heat-treated for 1 hour in the temperature range between 900-1080 °C. The zeolitic tuffs show endothermic peaks at about 100 °C and 200 °C, corresponding to dehydration of zeolitic water observed in the thermo- gravimetric curves and at ∼700 °C a small endothermic peak was identified corresponding to the structural breakdown of Phillipsite. According to the dilatometric traces, at about 870 °C, sintering of solid particles starts and a linear shrinkage of about 6% is reached at about 1050 °C. The maximum absolute and apparent densities were obtained after sintering at 1040 °C (absolute density = 2.59 g/cm^3; apparent density = 2.33 g/cm^3). Over this temperature, the sample heat-treated at 1060 °C, density results show a decreasing trend. The chemical composition of studied zeolitic tuffs make possible the liquid phase formation during heat-treatment, through the supplement of alkaline oxides. SEM image of the sample obtained at 1040 °C shows a zone with micro-crystallinity around the boundary of Sanidine grain highlighting the beginning of the phase transition from Sanidine, to Microcline. Heat-treatment effect of zeolitic tuff leads to the decomposition of Phillipsite and Sanidine and the formation of a new crystal phase of Hematite.

Keywords: Zeolitic tuff; sintering process; thermal behaviour; microstructural and phase transformations

1. Introduction

The high price of raw materials and their cost of transportation are important issues for ceramic manufacturing industries. The future development direction of ceramic industry is to maintain a high-end products and brands at the same time, more efforts should be made to the development of alternative raw materials for the production. Some studies were carried out using glass cullet [1–3], different industrial wastes [4,5] as well as some pyroclastic outcrops with acidic compositions as zeolite rich rocks [6–8]. The numerous applications recently found for volcanic tuffs [9–11] have increased the demand for fast and specific techniques, providing direct information on the components responsible most for their chemical and physicochemical behaviour.

Natural zeolites are currently being investigated widely for application of these rocks in various technologies, which contributes to industrial working of the deposits. The most topical research is oriented to using natural zeolites as local siliceous materials for such resource-consuming sectors as housing construction, and this concerns all silicate technologies: ceramic, glass, and binding materials [12–15]. These natural materials are abundant in many countries and having interesting ceramic properties by heat- treatment and consequently phase transformations [16]. Up to now, many studies have been reported technological features of natural zeolites such as low-melting temperatures, low-hardness and high-cation exchange capacity [17]. It has been shown that these natural materials undergo structural changes after heating which open possibilities to be used in different fields. [18–20]. The response to heating is an important aspect of natural zeolites, and the details of their thermal behaviour bear on

* Corresponding author. Dipartimento di Ingegneria Civile, Edile ed Ambientale, Sapienza-Università di Roma, Via Eudossiana, 18, 00186, Rome, Italy. Tel.: +39 0644585010; fax: +39 0644585016.
E-mail address: giuseppe.sappa@uniroma1.it (G. Sappa).

0272-8842/$36.00
doi:10.1016/j.ceramint.2011.03.048

topics ranging from industrial applications to their identification [21]. It is also mentioned that natural zeolite can be an alternative material to synthetic zeolite. But, the composition and properties of natural zeolites vary significantly from sample to sample Thus, before using a zeolitic tuff for a certain application its thermal and structural properties should be carefully investigated.

The cost of traditional raw materials used in porcelain production (i.e. clays, feldspar, quartz) is higher than that of zeolite. Moreover, feldspar and silica are both harder raw materials than zeolite and their crushing and millings are costly compared to zeolite [22,23]. On the base of the previous researches, the aim of the present study is the characterization of a Phillipsite rich natural zeolitic tuff and investigation of microstructural and phase transformations during sintering. The deposits of studied zeolitic tuffs, located in the Southern part of the Tenerife Island, are very abundant in this area and they are associated with the alteration of volcanic tuffs.

2. Experimental

The zeolitic tuff samples were selected especially from quarries that already active in this region and these areas are allowed by the regional low to mining and extract the large quantity of materials. The variations of chemical and mineralogical compositions of these materials are important features for their industrial applications therefore, we collected samples from different commercial places.

The raw material coming from three different locations, labeled as Pirs, CB1, and CB2, was initially crushed and milled by an Agatha mill and sieved under 63 μm to obtain green bodies. The chemical composition of raw materials was performed by XRF (Spectro XEPOS) and the results are shown in Table 1. The phase and mineralogical analyses of the parent materials were investigated by XRD technique and optical microscopy, respectively. The thermal behaviour of raw samples was investigated in a temperature range from 25 to 1300 °C by means of DTA technique (Linseiz L81) at heating rate of 10 °C/min using 100 mg powder samples. At the same temperature range, the weight changes of solid specimens were also recorded (TGA). The sintering behaviour of raw materials was evaluated at 10 °C/min heating rate by differential dilatometer (Netzsch 402 ED), using 10 mm × 4 mm × 4 mm mm ''green'' samples. The formation and/or the disappearance of crystalline phases during heat-treatment were investigated by XRD (Philips PW3050 apparatus) analyses with a Ni-filtered CuKα radiation over a range of 2θ angle from 5 to 70 degrees. The crystalline fraction formed was estimated by comparing the intensity of the amorphous halo in the spectra of each of studied samples with that of corresponding glass (obtained after re-melting at 1350 ∘C and water quenching [24]. This method is based on the assumption that the decrease in scattering intensity of the amorphous phase in partially crystallized samples is proportional to the amount of formed crystal phase [25,26]. ''Green'' samples were formed by pressing powders using polyvinyl alcohol as a binder, prismatic moulds and a compacting pressure of 150 MPa. Samples of 10 mm × 4 mm × 4 mm, were investigated for the sintering behaviour of raw materials by differential dilatometer (Netzsch 402 ED), at a heating rate of 10 °C/min. The heat treatment temperature ranges were decided on the basis of DTA investigation. On the contrary, samples of 10 mm × 10 mm × 8 mm were heat-treated at different temperatures in the range 900 -1080 °C, using 10 °C/min heating and cooling rates. The degree of crystallisation was evaluated on sintered samples via density measurements. The bulk (apparent) density was measured by a dry flow pycnometer (GeoPyc 1360). The skeleton (relative) and real (absolute) densities were measured by He displacement Pycnometer (AccuPyc 1330) [27] before and after milling. The heat-treated samples at different temperatures were milled below 53 μm for the evolution of absolute densities. The density results were used to determine total, closed and open porosities. The raw materials coming from different locations were investigated by means of Nicolet Nexus FTIR in transmission mode [28]. The samples were powdered in stainless steel ball mill; the fraction below 53 μm. A 2.5 mg powder sample was weighted and mixed in agata mortar with 500 mg KBr, dried at 120 °C for 24 h and then shaped in a 13 mm diameter and 1.3 mm thickness spherical tablet. The samples were dried at 150 C for 24 h and the spectra were collected in the 400–4000 cm^{-1} wave-number range. Scanning Electron Microscopy (Philips XL30CP) was employed to investigate the structure of the final samples, heat- treated in the range 900-1080 °C, using secondary electron, SE, and back scattered electron, BSE, techniques after polishing and etching (5 s with 2 wt.% HF).

Table 1
Chemical analysis of investigated zeolitic tuffs.

Wt %	Pirs	Cantos Blancos (CB1)	Cantos Blancos (CB2)
SiO_2	52.5 ± 0.07	55.2 ± 0.09	55.80 ± 0.08
Al_2O_3	14.00 ± 0.04	15.5 ± 0.06	15.6 ± 0.06
TiO_2	0.62 ± 0.01	0.59 ± 0.02	0.60 ± 0.03
Fe_2O_3	3.35 ± 0.04	3.26 ± 0.03	3.01 ± 0.001
CaO	1.32 ± 0.05	1.01 ± 0.02	0.85 ± 0.01
MgO	2.55 ± 0.07	1. ± 0.05	1.50 ± 0.02
K_2O	4.85 ± 0.01	4.3 ± 0.02	5.69 ± 0.01

3. Results and discussion

3.1. Characterization of raw materials

Many studies were reported about the chemical composition of zeolite rich rocks that they present different chemical features. Particularly, Chabazite and Phillipsite rich rocks are characterized a low SiO_2/Al_2O_3 ratio and remarkable amounts of K_2O, CaO and Fe_2O_3. On the contrary, Clinoptilolite rich rocks are richer in silica (∼68%) and poorer in aluminium, iron, alkaline and alkaline-earth oxides [17]. In our study, the chemical composition of the samples is characterized by high amount of SiO_2, 52÷55%, and Al_2O_3, 13÷15%, along with low amount of Fe_2O_3, 3÷3.5%, CaO, 0.8÷1.5%, MgO,1-2.5%, K_2O, 4.5÷6% and TiO_2, 0.6%. The samples present higher iron

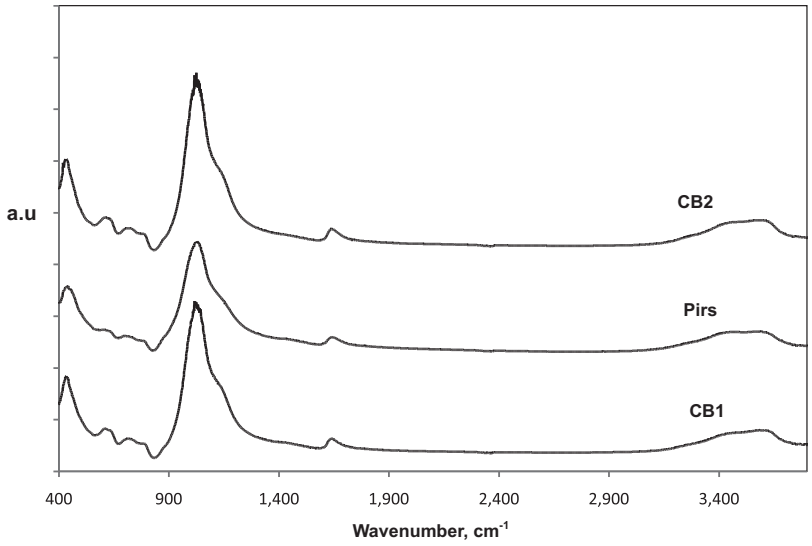

Fig. 1. The FTIR spectrum of natural zeolitic tuff.

content considering the traditional feldspathic fluxes utilized for ceramic industry ($Fe_2O_3 < 1\%$) [29]. From the chemical perspective, CB1 and CB2 samples do not show big differences in their compositions, however, Pirs sample shows lower $SiO_2 + Al_2O_3$ ratio (Table 1).

The mineralogical analysis demonstrated that zeolitic tuffs contain Sanidine minerals and Phillipsite microlites in an amorphous matrix. The high amount of glassy phase is due to the intensive eruption, followed by fast water cooling of the volcanic tuff formation.

The FTIR spectra of natural zeolitic tuffs show the most intense band at about 1100 cm^{-}, wave number corresponding to Si-O-Si asymmetric stretching vibration (Fig. 1). In the range 700-900 cm^{-1} bands relative to (Si,Al)-O stretching modes typical of Sanidine are observed. At 470 cm^{-1} wave number a band corresponding to the Si-O-Si asymmetric bending vibration is observed [30].

3.2. Thermal behaviour and sintering behaviour of zeolitic tuff

In Fig. 2 the thermo gravimetric curves of CB1, CB2 and Pirs samples are reported. In three samples, weight losses of 2-3.3% has been observed until about 220 °C, corresponding to the endothermic peaks observed in the dilatometer. In the range 220-650 °C the samples show further weight reduction of 0.2-0.8%. Above this temperature, corresponding to the contraction of the zeolite structure, the weight is constant for all the samples. The DTA traces of zeolitic tuffs show endothermic peaks at about 100 °C and 200 °C, corresponding to dehydration of zeolitic water observed in the thermo gravimetric curves. At ~700 °C a small endothermic peak was identified corresponding to the structural breakdown of Phillipsite [31]. The DTA traces also show a strong endothermic effect starting at 900 °C with a peak temperature over than 1200 °C (Fig. 2).

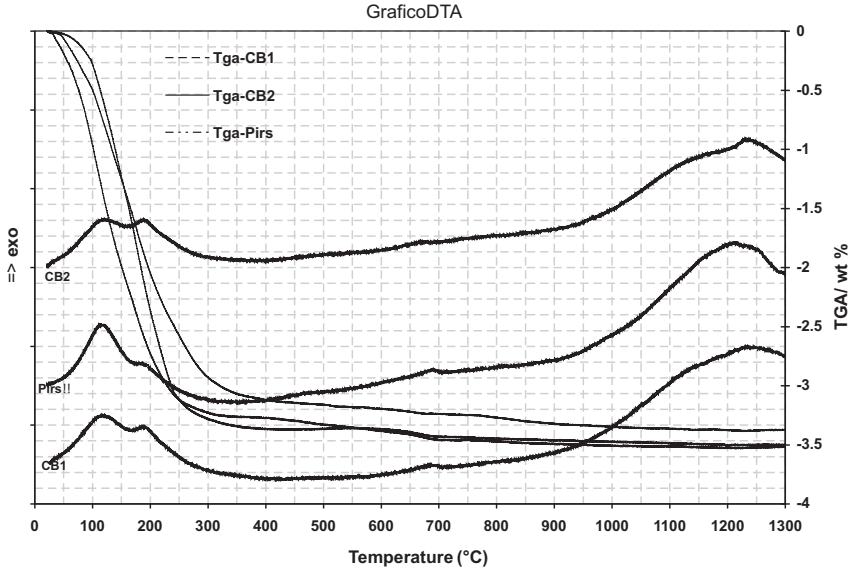

Fig. 2. TGA and DTA curves of zeolitic tuff.

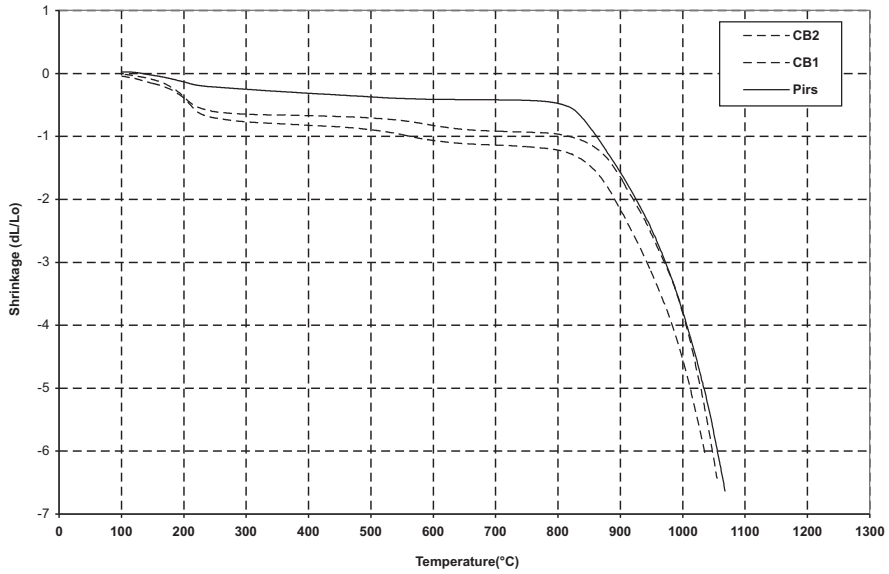

Fig. 3. Dilatometric traces of zeolitic tuffs.

This is probably due to the melting of the crystal phases present in the tuffs.

Densification phenomenon always led to shrinkage of the ceramic body during heating (i.e. firing shrinkage) [32]. It is very well known that firing shrinkage is a measure of densification during heat-treatment and depends basically on the composition of the raw materials, particle size distribution, sintering time and temperature [33]. The sintering behaviour of the studied zeolitic tuffs was evaluated by thermal dilatometer with 10 °C/min heating rate. Fig. 3 reports the linear shrinkage of the samples, $\Delta L/L_0$, as a function of temperature. Previous studies related to densification of zeolitic tuffs show that Chabazite–Phillipsite materials, rich in iron oxide, demonstrates lower sintering temperatures that are similar to nepheline syenite, while Clinoptilolite compositions are slightly less fusible, with characteristic temperatures similar to sodic feldspar [34,35]. In our study, at about 220 °C, a 0.8% linear contraction was measured in the correspondence of the dehydration of zeolite. In the range 220-650 °C, samples show further shrinkage (0.5-1.1%). This can be related the structural breakdown of the Phillipsite. Above about 870 °C, sintering of solid particles starts and a linear shrinkage of about 6% is reached at about 1050 °C. Over this temperature the linear shrinkage tends to increase. The larger shrinkage of these bodies is probably explained by an increase of both the liquid phase during the viscous flow sintering and the porosity formed during heat treatment. The chemical composition of studied zeolitic tuffs make possible the liquid phase formation during heat-treatment, through the supplement of alkaline oxides. These oxides decrease melting temperature of powder and facilitate fusibility leading liquid phase sintering.

Based on the preliminary results the samples labeled as Pirs, CB1 and CB2 were considered similar. Therefore, CB1 sample was selected for subsequent heat-treatment process to synthesize microstructural and phase transformations during sintering.

As mentioned above, the sintering behaviour of the batch, prepared using only milled zeolitic tuff, was evaluated by thermal dilatometer. However, to understand better the sintering effect, hot-stage microscopy techniques was applied mixing the zeolitic tuff with some clays and feldspars (20% zeolitic tuff, 40% clays, 40% feldspars). In Fig. 4 the hot- stage microscopy images of the batch are presented. According to the results, the sample shows the beginning of sintering about 1130 °C and deformation after ∼ 1160 °C showing lower sintering temperature than the porcelain stoneware tiles.

The densification of the samples was estimated by measuring the variation of apparent, ρb, skeleton, ρs, and absolute, ρr, densities (Table 2). Density measurements are consistent with the shrinkage values and the sintering behaviour. The maximum absolute and apparent densities were obtained after sintering at 1040 °C (absolute density = 2.59 g/cm^3; apparent density = 2.33 g/cm^3). Nevertheless, further heating lowers the values of density but increases the size and number of the pores. The decreasing trend of density above this temperature related to the evolution of gaseous phases generating closed porosity inside the samples because of high amount of silica and alkaline content of the batch and/or can be attributed to the O_2 release from the reduction of Fe_2O_3 [36]. This is resulting in self-glazing of the body surface during sintering. In fact, a strong self-glazing effect was found above 1040 °C, however, increasing the temperature caused deformation of the shape of pellets and decrease in density due to the formation of pores.

Based on the density measurements, total, closed and open porosities were evaluated with the following equations PT = 100*[(ρr − ρb)/ρr], PC = 100*[(ρr − ρs)/ρr], PHe = PT-PC, respectively, and the results were plotted in Fig. 5 At 900 °C the closed porosity resulted to be negligible and the total porosity is about 32% highlighting a no remarkable densification. At 1000 °C total and open porosities extremely decrease with the value ∼ 9,5% and ∼ 8,4% respectively. At 1040 °C

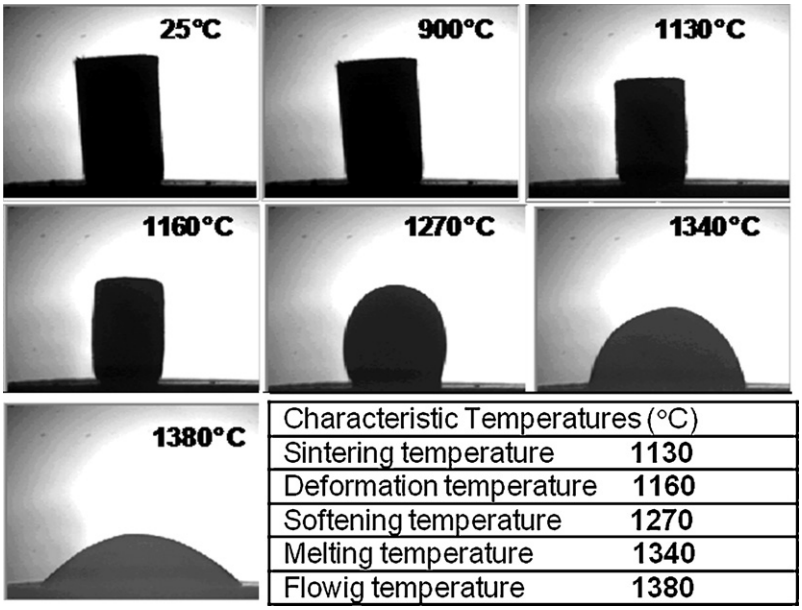

Fig. 4. Heating microscopy images of the batch.

Table 2
Density and porosity of green and sintered samples.

Temperature (°C)	Apparent density (g/cm^3)	Skeleton density (g/cm^3)	Absolute density (g/cm^3)	Total porosity (%)	Close porosity (%)	PO_{He}
20	1.356	2.236	2.250	39.70	0.63	39.00
900	1.736	2.549	2.569	32.40	0.78	31.60
1000	2.329	2.546	2.577	9.62	1.20	8.40
1040	2.335	2.392	2.597	10.00	7.89	2,20
1060	2.252	2.334	2.584	12.80	9.67	3.20
1080	2.131	2.358	2.579	17.30	8.57	8.80

total porosity remains at about the same value, however open porosity reduces and closed porosity takes place with the value of ∼ 7,8%. At 1060 °C the total porosity starts to increase in parallel with open and close porosities showing the beginning of deformation. Finally, at 1080 °C total porosity reaches to ∼ 17% and the open porosity increases to 8.8% and the closed porosity decreases to 9.6% indicating an over- firing process.

X-Ray patterns of the zeolitic tuff samples were analyzed considering the peaks within the 5° and 70° 2(range. In Fig. 6 spectra of natural, CB1, and heat treated materials, has been

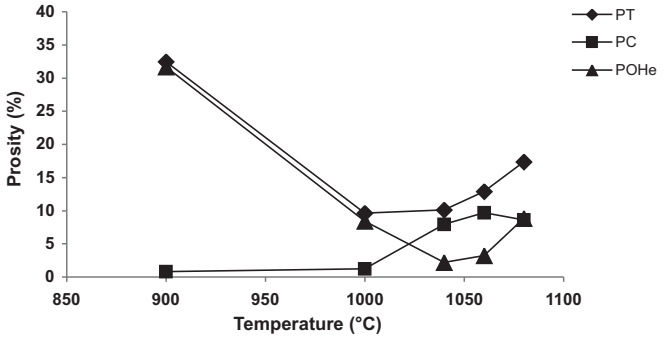

Fig. 5. Total porosity (PT), close porosity (PC), and open porosities for He (PHe) of the sintered samples.

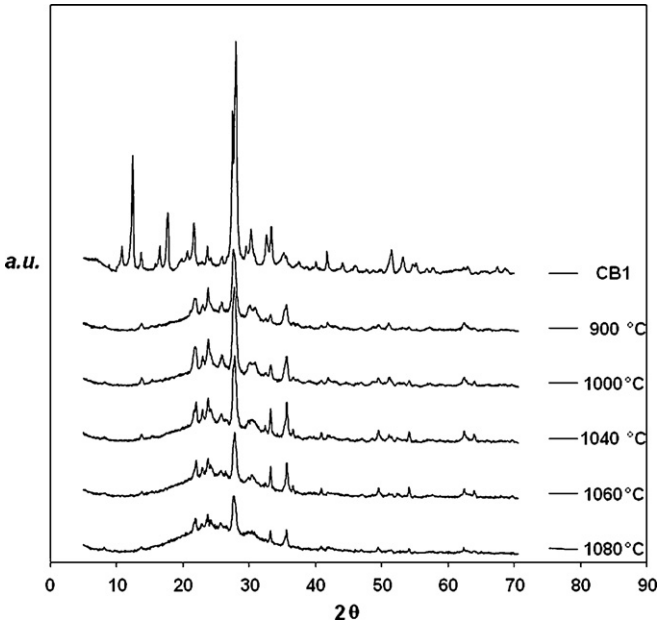

Fig. 6. The XRD diffraction patterns of natural zeolitic, CB1, tuff and heat-treated samples at (a) 900 °C; (b) 1000 °C; (c) 1040 °C; (d) 1060 °C; (e) 1080 °C.

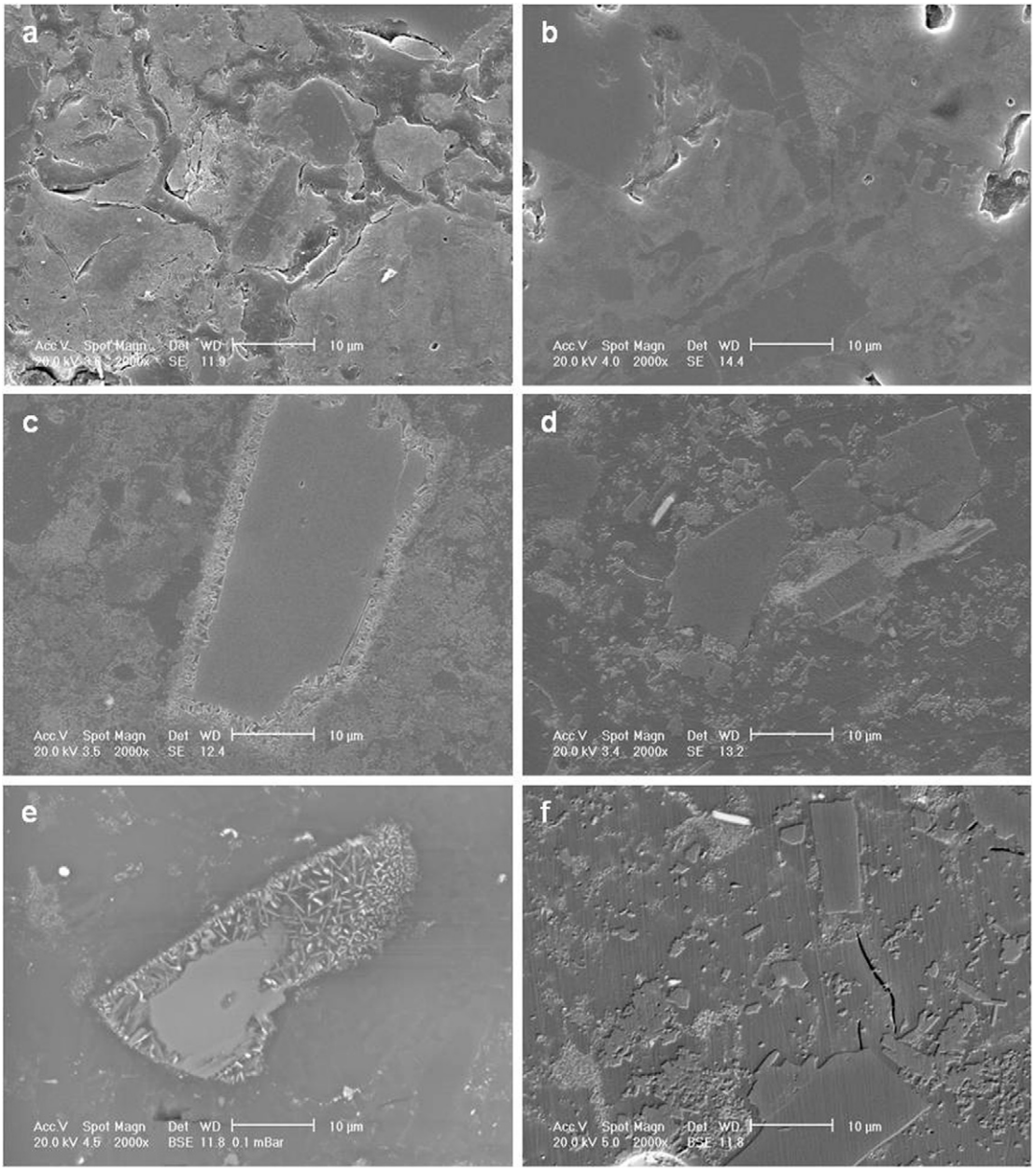

Fig. 7. Scanning electron microscopy images of the sintered products: (a) 900 °C; (b) 1000 °C; (c) 1040 °C; (d) 1060 °C; (e,f) 1080 °C.

reported. Natural zeolitic tuff shows about 70% crystal phase being Phillipsite, main peak at $2\theta = 12.5^{\circ}$, Sanidine, $2\theta = 27.5^{\circ}$, and Plagioclases, $2\theta = 28^{\circ}$. The samples heated up to 900-1040 °C show about 50% amorphous phase, due to the complete destruction of Phillipsite crystal structure and the decreasing of Plagioclases and Sanidine. As a new phase, Hematite (peak at $2\theta = 33.2$ degrees) was detected. In the sample heat treated at 1060 °C, the amorphous phase increase to about 60%, due to the melting of crystal phases, and, finally, the sample sintered at 1080 °C shows 70% amorphous phase. At the temperatures of 1060 °C and 1080 °C, the amount of Hematite decreased.

Microstructural investigations of sintered products were carried out using scanning electron microscopy techniques. Fig. 7 presents SEM micrographs, from the surface, of the samples heat-treated at 900 ÷ 1080 °C. In Fig. 7 (a) the crystals and fractured structure were present in the sample heat-treated at 900 °C and this fact was consistent with the porosity and density measurements showing a low degree of sintering. At 1000 °C, Fig. 7 (b), the microstructure is more homogeneous. This fact indicates that increasing the temperature facilitates liquid phase sintering mechanism. In Fig. 7 (c), the SEM image of the sample obtained at 1040 °C shows a zone with micro-crystallinity around the boundary of Sanidine grain, at the interface with a glassy matrix, highlighting the beginning of the phase transition from Sanidine, to Microcline, i.e. from monoclinic to triclinic crystal system. In Fig. 7 (d), sample heat-treated at 1060 °C, the surface is characterized by a more fine-crystalline morphology, however in this temperature density results show a decreasing trend due to the evolution

of gaseous phases generating closed porosity inside the samples. Finally, at 1080 °C, Fig. 7 (e-f), the Microcline formation takes place intensively and the Sanidine stays in the center of the new – formed crystal matrix. In addition, the high crystallinity of sample, as well as the presence of different crystal phases is evident on the surface, nevertheless the high percentage of closed porosity of this sample is not confirm a good degree of sintering.

4. Conclusion

In this study a Phillipsite rich zeolitic tuff from Tenerife, Canary Islands, was characterized for chemical composition, structure and thermal behaviour. The heat- treatment conditions for maximum densification and minimum porosity formation were assessed: a sintering temperature of 1040 °C and a dwell time at this temperature of 1 h. Under these conditions this sample characterized closed and open porosities with the value of 7,8% and 2,2%, respectively. Over this temperature, the decrease of the densities and increase of the total porosities may be related to the evolution of gaseous phases generating closed porosity inside the samples because of high amount of silica and alkaline content of the batch and/or can be attributed to the O_2 release from the reduction of Fe_2O_3. The weight loss is mostly associated with the dehydration of zeolite minerals as well as oxidation during heat-treatment that contributes to increase the porosity and the linear shrinkage thus, it can be create technological problems during production. Hot-stage microscopy analysis of the powder, obtained by mixing 20% zeolitic tuff, 40% clays and 40% feldspars, shows the beginning of sintering at about 1130 °C and deformation after $\sim$ 1160 °C highlighting lower sintering temperature than the porcelain stoneware tiles. Heat-treatment effect of zeolitic tuff leads to decomposition of Phillipsite and Sanidine, while the formation of a new crystal phase of Hematite. The use of zeolitic tuffs as alternative raw materials in the ceramic industry gives the advantage of reducing the energy consumption thanks to easy grinding ability and lower sintering temperature respect to other fluxes [37]. Regulating heat-treatment process, zeolitic tuff deposits in this area can be considered as an important raw material for different applications in technological areas.

Acknowledgements

The authors wish to thank Assoc. Prof. Jose Miguel Caceres for his technical support and kind invitation to the University of La Laguna, Tenerife, Canary Islands.

References

[1] A. Tucci, L. Esposito, E. Rastelli, C. Palmonari, E. Rambaldi, Use of sodalime scrap-glass as a fluxing agent in a porcelain stoneware tile mix, Journal of European Ceramic Society 24 (2004) 83–92.
[2] G. Garbonchi, M. Dondi, N. Morandi, F. Tateo, Possible use of altered volcanic ash in ceramic tile production, Industrial Ceramics 19 (1999) 67–74.
[3] F. Matteucci, M. Dondi, G. Guarini, Effect of soda-lime glass on sintering and technological properties of porcelain stoneware tiles, Ceramics International 28 (2002) 873–880.
[4] F. Andreola, L. Barbieri, A. Corradi, I. Lancellotti, T. Manfredini, Utilisation of municipal incinerator grate slag for manufacturing of porcelainized stoneware tiles manufacturing, Journal of European Ceramic Society 22 (2002) 1457–1462.
[5] A. Karamanov, E. Karamanova, A.M. Ferrari, F. Ferrante, M. Pelino, The effect of scrap addition on the sintering behaviour of hard porcelain, Ceramics International 32 (2006) 727–732.
[6] R. de' Gennaro, P. Cappelletti, G. Cerri, M. de' Gennaro, M. Dondi, A. Langella, Zeolitic tuffs as raw materials for lightweight aggregates, Applied Clay Science 25 (2004) 71–81.
[7] K. Dana, S. Das, S.K. Das, Effect of substitution of fly ash for quartz in triaxial kaolin–quartz–feldspar system, Journal of European Ceramic Society 24 (2004) 3169–3175.
[8] P. Torres, H.R. Fernandes, S. Agathopoulos, D.U. Tulyaganov, J.M.F. Ferreira, Incorporation of granite cutting sludge in industrial porcelain tile formulations, Journal of European Ceramic Society 24 (2004) 3177–3185.
[9] F.A. Mumpton, La roca magica: Uses of natural zeolites in agriculture and industry, 96, National Academy of Sciences, U S A., 1999, 3463-3470.
[10] E.J. Kogel, N.C. Trivedi, J.M. Barker, S.T. Krukowski, Industrial Minerals & Rocks, Commodities, in: Markets and Uses, 7th ed., SME: Littleton, CO, 2006.
[11] E. Passaglia, Zeoliti naturali, zeolititi e loro applicazioni, Arvan, Venice, Italy, 2008.
[12] V.N. Smirenskaya, V.I. Vereshchagin, Prospects of using zeolite rocks of Siberia in silicate materials, Glass and Ceramics 59 (2002) 414–419.
[13] G.I. Ovcharenko, V.L. Sviridov, L.K. Kazantseva, Zeolites in Construction Materials, Izd-vo AltGTU, Barnaul, 2000, [in Russian].
[14] V.M. Pogrebenkov, E.D. Mel'nik, V.I. Vereshchagin, The use of mineral materials of Siberia in the production of self-glazing ceramic tiles, Glass and Ceramics 54 (11–12) (1997) 373–375.
[15] G. R. Vagner, N.N. Kruglitskii, and V. G. Tikhonov, Prediction of the efficiency of using zeolite minerals in cement for various purposes, in: Proc. XIV Conference of Silicate Industry and Science, Budapest (1985), 307–314.
[16] O. San, S. Abalı, C. Hosten, Fabrication of microporous ceramics from ceramic powders of quartz–natural zeolite mixtures, Ceramics International 29 (2003) 927–931.
[17] R. Gennaro, P. Cappelletti, G. Cerri, M. Gennaro, M. Dondi, G. Guarini, A. Langella, D. Naimo, Influence of zeolites on the sintering and technological properties of porcelain stoneware tiles, Journal of the European Ceramic Society 23 (2003) 2237–2245.
[18] O.C. Duvarcı, Y. Akdeniz, F. Ozmihci, S. Ulku, D. Balkose, M. Ciftcioglu, Thermal behaviour of a zeolitic tuff, Ceramics International 33 (2007) 795–801.
[19] D.W. Breck, Zeolite Molecular Sieve; Structure, Chemistry And Use, John Wiley and Sons, New York, 1974.
[20] G. Cruciani, Zeolites upon heating: Factors governing their thermal stability and structural changes, Journal of Physics and Chemistry of Solids 67 (2006) 1973–1994.
[21] D.L. Bish, J.W. Carey, Thermal Behaviour of Natural Zeolites, in: D.L. Bish, D.W. Ming (Eds.), Natural Zeolites: Occurrence, Properties, Applications. Mineralogical Society of America Reviews in Mineralogy and Geochemistry, 45, 2001, pp. 403–452.
[22] S.P. Chaudhuri, P. Sarkar, Dielectric behaviour of porcelain in relation to constitution, Ceramics International 26 (2000) 865–875.
[23] K.H. Schüller, Porcelain: Ceramics Monographs–Handbook of Ceramics, Verlag Schmidt GmbH, Freiburg Germany, 1979.
[24] Z. Strand, Glass ceramic materials, Glass and Technology, 8, Elsevier, Amsterdam, 1986.
[25] A. Karamanov, S. Ergul, M. Akyildiz, M. Pelino, Sinter-crystallization of a glass obtained from basaltic tuffs, Journal of Non-Crystalline Solids 354 (2008) 290–295.
[26] H.S. Kim, R.D. Rawlings, P.S. Roger, Quantitative determination of crystalline and amorphous phases in glass-ceramics by X-ray diffraction analysis, British Ceramic Transactions and Journal 88 (1989) 21–25.

[27] http://www.micromeritics.com
[28] P. Pisciella, M. Pelino, FTIR spectroscopy investigation of the crystallization process in an iron rich glass, Journal of the European Ceramic Society 25 (2005) 1855–1861.
[29] M. Dondi, Compositional Parameters to Evaluate Feldspathic Fluxes for Ceramic Tiles, Tile & Brick International 10 (1992) 77–84.
[30] W. Mozgawa, The relation between structure and vibrational spectra of natural zeolites, Journal of Molecular Structure 596 (2001) 129–137.
[31] B.S. Hemingway, R.A. Robie, Thermodynamic Properties of Zeolites: Low-Temperature Heat Capacities and Thermodynamic Functions for Phillipsite and Clinoptilolite. Estimates of the Thermochemical Properties of Zeolitic Water at Low Temperature, American Mineralogist 69 (1984) 692–700.
[32] A. Roy, S.K. Singh, P.C. Banerjee, K. Dana, S. Das Kumar, Biobeneficiation of kaolin and feldspar and its effect on fired characteristics of triaxial porcelain, Bulletin of Material Science 33 (2010) 333–338.
[33] A. Salem, S.H. Jazayeri, E. Rastelli, G. Timellini, Dilatometric study of shrinkage during sintering process for porcelain stoneware body in presence of nepheline syenite, Journal of materials Processing Technology 29 (2009) 1240–1246.
[34] R. de Gennaro, M. Dondi, P. Cappelletti, G. Cerri, M. de' Gennaro, G. Guarini, A. Langella, L. Parlato, C. Zanelli, Zeolite–feldspar epiclastic rocks as flux in ceramic tile manufacturing, Microporous and Mesoporous Materials 105 (3) (2007) 273–278.
[35] M. Dondi, G. Guarini, I. Venturi, Assessing the fusibility of feldspathic fluxes for ceramic tiles by hot stage microscope, Industrial Ceramics 21 (2001) 67–73.
[36] M.J. Ortz, A. Escardino, J.L. Amoròs, F. Negre, Microstructural Changes During the Firing of Stoneware Floor Tiles, Applied Clay Science 8 (n. 2–3) (1993) 193–205.
[37] A.G. Ashmarin, A.S. Vlasov, Science for ceramic Production, Wall ceramics from zeolite-bearing argillaceous materials, Glass and Ceramics 62 (9–10) (2005) 14–16.